

Design and optimization of microlens array based high resolution beam steering system

Ata Akatay and Hakan Urey

Department of Electrical Engineering, Koc University, Sariyer, Istanbul 34450, Turkey
hurey@ku.edu.tr

Abstract: High-resolution imaging and beam steering using 3 microlens arrays (MLA) is demonstrated. Small lateral displacement of one microlens array is sufficient for large angle beam steering. A prescan lens is added to the system to overcome the discrete addressing problem associated with microlens scanning systems. A hybrid method that uses both geometrical ray tracing optimization and physical optics simulation is introduced for the design and optimization of the MLA system. Feasibility of 1880×1880 resolution using $f/2$ aspherical MLAs and 752×752 resolution using $f/5$ spherical MLAs are demonstrated assuming 100 μ m microlens pitch and 2mm clear aperture. The system is compact and suitable for endoscopic imaging and agile steering of large beams.

©2007 Optical Society of America

OCIS codes: (050.0050) Diffraction and gratings; (080.2740) Geometrical optics, optical design; (120.5800) Scanners; (170.3890) Medical optics instrumentation; (220.4830)

References and links

1. J. Duparré, D. Radtke, and P. Dannberg, "Implementation of Field Lens Arrays in Beam-Deflecting Microlens Array Telescopes" *Appl. Opt.* 43, 4854-4861 (2004).
2. A. Akatay, C. Ataman, and H. Urey, "High-resolution beam steering using microlens arrays," *Opt. Lett.* 31, 2861-2863 (2006).
3. J. W. Goodman, *Introduction to Fourier Optics* (McGraw-Hill, 1996).
4. H. Urey, "Retinal Scanning Displays," in *Encyclopedia of Optical Engineering*, R. Driggers, ed., (Marcel Dekker, 2003), pp. 2445-2457.
5. J. Sun, L. Liu, Y. Maojin, and W. Lingyu, "Study of the transmitter antenna gain for intersatellite laser communications" *Opt. Eng.* 45, 58001- 58006 (2006).
6. M. Born and E. Wolf, *Principles of Optics*, seventh ed., (Cambridge University Press, 2002)
7. Software for Optical Design; Zemax Development Corporation (2006).
8. N. Lindlein, "Simulation of micro-optical systems including microlens arrays," *J. Opt. A: Pure Appl. Opt.* 4, 1-9 (2002).
9. H. Urey, N. Nestorovic, B. Ng, and A. Gross, "Optics Designs and System MTF for Laser Scanning Displays," *Proc. SPIE* 3689, 238-248 (1999).
10. N. F. Borrelli, *Microoptics Technology: fabrication and applications of lens arrays and devices*, (Marcel Dekker, 1999).
11. A. Akatay, A. Waddie, H. Suyal, and M. Taghizadeh, and H. Urey "Comparative performance analysis of 100% fill-factor microlens arrays fabricated by various methods," *Proc. SPIE* 6185, 1-11 (2006).

1. Introduction

Development of new fabrication technologies paves the way for applications of microlens arrays (MLAs) such as in optical interconnection, wavefront detection, and imaging systems. The MLA beam steering system is essentially a telescope system where the beam is scanned by the relative lateral motion of the two MLAs separated by twice their focal length. In order to prevent spurious light leaks when the MLA is displaced, a field MLA (2nd MLA) is added in between the other two MLAs as discussed in Ref. [1]. The scheme is quite attractive as large scan angles can be achieved by small displacements. However, the concept has a major limitation, that is only discrete scan angles corresponding to diffraction order angles are

addressable due to the periodic structure of the MLAs. The discrete addressing limitation can be overcome by using a prescan lens (PSL) before the MLAs, continuous addressing with limited resolution was demonstrated and the results were recently reported by the authors [2].

In this paper, design and optimization of the MLA based beam steering systems with high resolution (1880×1880) and diffraction-limited performance is reported using $f/2$ aspherical MLAs. Major contribution of this paper is in the demonstration of diffraction-limited 2-point resolution performance using $f/2$ lenses and beam steering angles as large as ± 0.25 rad. Such high-resolution can be achieved using small arrays and small deflections, thus, high-speed beam steering is possible. While the paper is focused on angular beam steering, high resolution imaging can be accomplished by simply adding a large field-of-view focusing lens after the afocal telescopic system.

A method for optimization of the system is developed where a single channel of the cascaded MLAs is optimized. The optimization is carried out with ZemaxTM using multi-configurations and a special merit function, which is defined to optimize both the aberration and array performance. Performances of optimized systems utilizing $f/2$ and $f/5$ aspherical and $f/5$ spherical MLAs are reported. The results are compared with the experimental system utilizing $f/5$ spherical MLAs in Section 5.

2. System analysis

MLA beam steering systems are telescopic array systems, and array of collimated beamlets are output from an array of microlenses. The far-field pattern is the result of interference of these beamlets. Constructive interference is satisfied by a pre-scanning lens (PSL) prior to the telescope system as illustrated in Fig. 1 [2]. The imaging lens provide focusing and the collection fibers collect the scattered light from the object surface. The illustration is suitable for a laser camera system which can fit in a 5mm endoscopic surgery tube.

The telescope system can be analyzed as identical channels which are composed of a train of three microlenses. For the convenience of analysis without loss of generality we will analyze the system in one dimension and use the special functions such as rect, comb, sinc as defined in Ref. [3]. Extension of the analysis into two dimensions is straightforward. The transmission function of the system at the output of the 3-MLA channel assuming collimated beam incidence can be shown to be a periodical phase function:

$$t(x) = [A(x) \exp(-i\alpha(x)) \text{rect}(x/a)] * [(1/d) \text{comb}(x/d) \text{rect}(x/D)] \quad (1)$$

where d is the MLA pitch, D is the clear aperture size, $\alpha(x)$ is the phase appearing on each microlens channel and equal to the sum of the wavefront aberration, $\phi(x)$, and a linear tilt term due to the MMLA displacement. D is equal to $N.d$, where N is the array size in one dimension. $A(x)$ is the amplitude distribution function across each MLA, and $a \leq d$ is the beamlet diameter at the output of each MLA channel as defined in Fig. 1. The field distribution at the image plane -the point spread function (PSF), is obtained by the Fourier transform of the $t(x)$:

$$I(\theta) = (aD)^2 \left[\mathcal{F} [A(x) \exp(-i\alpha(x)) \text{rect}(x/a)] \right]^2 \times [\text{comb}(d \sin \theta / \lambda) * \text{sinc}(D \sin \theta / \lambda)] \quad (2)$$

The equation is a multiplication of two terms: a wide envelope Sinc function (I_1) and a train of narrow sinc functions (I_2), as shown in Fig. 2. If there are no aberrations (i.e. $\phi(x)=0$), and the irradiance distribution across each microlens is uniform (i.e., $a=d$ and $A(x)=1$), the Fourier transform simplifies to $\text{sinc}[(d/\lambda) \sin \theta]$, and the zeros of I_1 overlaps with the higher order diffraction peaks of I_2 and would yield irradiance zeros at those points. In case of aberrations and/or non-uniform irradiance distribution across each microlens of MLA3, the envelope Sinc function denoted by I_1 widens and higher order diffraction peaks of I_2 appears in the PSF, as illustrated in Fig. 2. When the system has small amount of aberrations, almost all of the

optical energy is distributed inside the main lobe of I_1 (e.g., within the 0th and +/-1st order diffraction lobes of I_2) and the energy outside the main lobe is negligible. In general, $A(x)$ can be assumed uniform and the aberrations can be calculated as wavefront deviation from a reference wavefront.

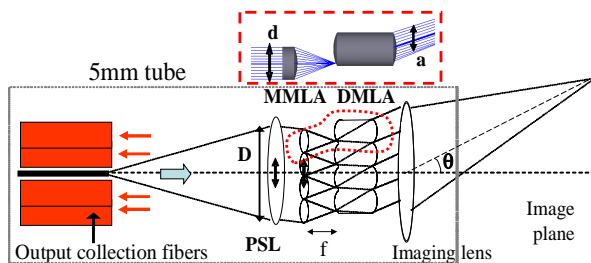


Fig. 1. System geometry and steering of light by displacements of the PSL and MMLA.

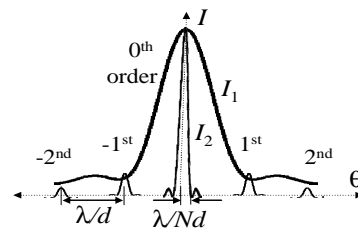


Fig. 2. Illustration of the PSF composed of a train of Sinc functions (I_2) under a Sinc-like envelope function (I_1), where $D=Nd$.

The resolution of the optical system is determined by the total scan angle divided by the minimum angular width of the 0th order Sinc function in I_2 , which can be taken as λ/D . It is interesting to note that as long as the aberration function is periodic, the 0th order diffraction spot size, thus the angular resolution of the system, remain the same independent of the aberrations and the microlens fill-factor. The width of a single diffraction order always remain proportional to λ/D , thus remain diffraction limited. However, distribution of energy to different diffraction orders is affected by the aberrations, reducing the contrast of the imaging system, but not the two-point resolution. This is a unique property and important advantage of MLA scanning systems compared to scanning with mirrors or spatial phase modulators [4, 5].

3. Optical performance metrics for analysis and optimization

Modulation transfer function (MTF) of the system can be utilized for evaluation of the spurious light (i.e. high order diffraction lobes) in the MLA scanner system. MTF of a system is equivalent to the autocorrelation of the system transmission function $t(x)$. [3] Hence, for the best system performance a perfectly uniform field is desired at the output. Deviations from the perfect uniform field can be analyzed separately as amplitude and phase deviations. In the design cases reported in this work, a uniform amplitude distribution is enforced, hence in the analysis only phase related wave aberrations are considered.

Wave aberrations reduce the *peak-to-sidelobe ratio*, which can be defined as the ratio of the peak intensities of the mainlobe and the sidelobe of the PSF. Similarly, the Strehl ratio (V) which is defined as the ratio of the PSF peak intensity of the aberrated system to that of an unaberrated diffraction-limited system, can be used as a measure for evaluation of the optical energy in the central lobe compare to the energy in the spurious sidelobes. The Strehl ratio of the system can be determined from the area integral of the phase function for the aberrated and the unaberrated cases, which correspond to the ratio of the Fourier transforms evaluated at the zero frequency. If the system is slightly aberrated ($V>0.5$), V can be expressed as $V = 1 - (2\pi\sigma)^2$, [6], where σ is the RMS wavefront error and can be obtained from ray tracing optical design tools such as ZemaxTM. [7]

4. Simulation and optimization of the system

Propagation of the beamlets through the three microlenses can be analyzed using ray tracing software. In the literature there are methods for considering both the diffraction and the aberration effects, [8] however, we first focus optimization of the wavefront error function $\phi(x)$. In case of uniform illumination and where MLAs are identical, the simulation and optimization of the whole system can be reduced to the analysis of a single channel of microlenses. Replication of the single channel wavefront error across the array gives $\phi(x)$. In the final step, the wavefront after the MLAs can be constructed using $\phi(x)$ and propagated to the far-field by a 2D Fourier transformation and scaling. The simulation of the system is illustrated in Fig. 3. The plane wave propagation between the DMLA and the imaging lens is skipped since an optimized imaging lens is assumed.

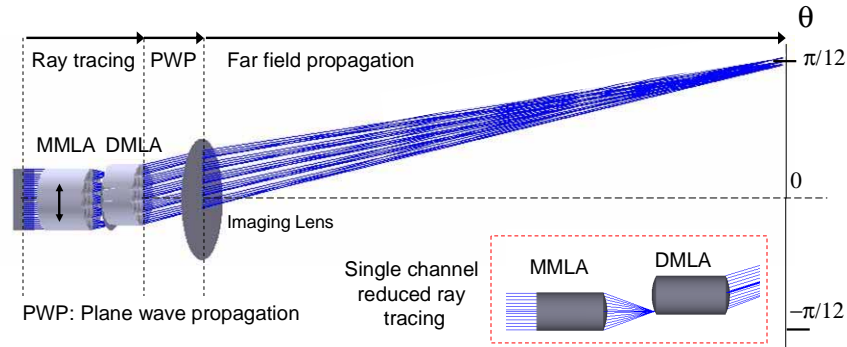


Fig. 3. 3D schematic view of the optimized system utilizing aspherical $f/2$ MLAs. Illustrating the propagation steps and the corresponding simulation methods.

In defining the optimization merit function (the cost function) the system performance is evaluated using the Strehl ratio as the main design criteria. As discussed in the previous section, in case of a uniform plane wave illumination, the peak-to-sidelobe ratio can be optimized by optimizing the Strehl ratio. In the optimization of the system, a slight amount of spurious light with less than 5% energy is allowed and the system is constrained to have uniform field distribution after the last microlens. Care should be taken to constrain the focused spot size at the second microlens and the maximum deflection to prevent light leaking into the neighboring microlenses. The merit function includes five configurations for the MMLA deflections given as: 0 , $\pm 0.25d$ and $\pm 0.425d$ and constrained to produce the desired beam steering angles subjected to lens curvature and thickness constraints.

In the optimization process the system variables are the lens profile parameters for each MLA surface and the distances between the surfaces, the imaging and the prescan lenses are not part of the optimization. The optimization is carried out for spherical and aspherical MLAs with f -numbers ($f_{\#}$) of 2 and 5. Since the wafer thickness can be larger than the focal length for the fast $f_{\#}$ systems, the MMLA curved surface faces the DMLA, even though aberration performance would be better otherwise. Figure 4 shows the optimized wavefront aberration plots in x/y directions across the microlens aperture obtained for various lens profiles for the maximum scan angle case, which is the worst case for this system, i.e. on-axis aberrations are negligible. All cases, except the one using spherical $f/2$ microlenses produce diffraction limited performance and high Strehl ratio.

The PSF of the optimized system is calculated by farfield propagation of the wavefront after the MLAs. In Fig. 5, the PSF of the system utilizing $f/2$ aspherical/spherical lenses are shown for two scan positions. Note that the main lobe widths are the same, while the energy shifted to diffraction rings are different, proving that the aberrations do not reduce the two-point resolution of the system but reduce the contrast at low spatial frequencies.

In Fig. 6, MTF is plotted for various configurations and in two scan conditions. The x-axis of the plots are in units of number of cycles (or linepairs) in a diffraction order separation ($\theta_d = \lambda/d$). Spatial cut-off frequency of the system is equal to $N/2$ cycles/ θ_d , which corresponds to a resolution of N pixels in a diffraction-order separation. [9] In all the reported cases in Fig. 6, except the $f/2$ -spherical configuration, the system performs nearly diffraction limited.

The overall resolution of the system in each axis can be obtained by multiplying the resolution per diffraction order (i.e. N), by the number of diffraction orders (NDO) across the scan line, which is equal to $2d\theta_{max}/\lambda$. The result gives the diffraction limited resolution i.e. $2Nd\theta_{max}/\lambda$. For $f/2$ and $f/5$ systems, the maximum beam steering angles are 0.25 rad and 0.1 rad. If $\lambda=0.532 \mu\text{m}$ and $N.d=D=2\text{mm}$ are assumed, a 2D resolution of 1880×1880 for $f/2$ aspherical MLAs and 752×752 for $f/5$ spherical MLAs can be obtained .

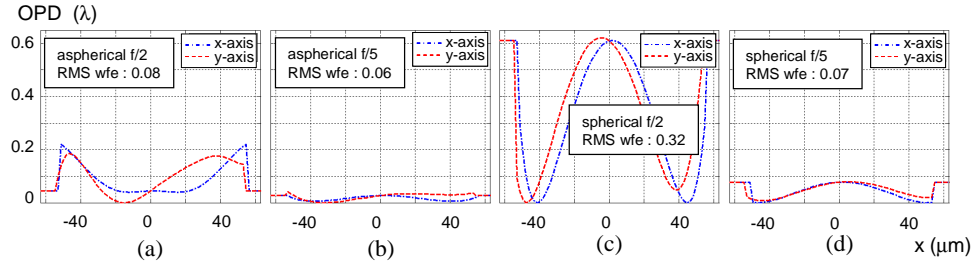


Fig. 4. X-Y axis cross sections of wavefront maps $\phi(x)$ of the systems at the maximum scan angle position for $100\mu\text{m}$ pitch MLAs with profiles: (a) aspherical $f/2$ (b) aspherical $f/5$ (c) spherical $f/2$ (d) spherical $f/5$. (RMS values are in number of wavelengths across square-shaped lens surface.)

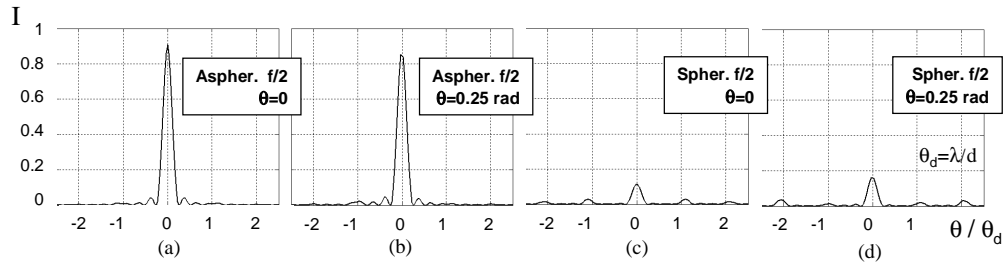


Fig. 5. Cross sections of the PSF, simulated for $f/2$, aspherical/spherical MLAs at the center and the maximum scan angle cases.

Nearly 100% fill-factor microlens arrays can be batch fabricated using a number of replication techniques or by photoresist melting. Replication molds can be fabricated using isotropic etching techniques for spherical profile and laser writing or gray-scale lithography for aspherical profile [10, 11]. If the actuator is to be retrofitted in a micromachined stage and fitted in a 5 mm tube, as illustrated in Fig. 1 for the endoscopic imaging application, a practical limit for the clear aperture is 2 mm.

5. Experimental system

The MLA scanner system is built using identical square packed, 100% fill-factor, $200 \mu\text{m}$ pitch, $f/5$ MLAs. The MLAs are illuminated by a beam of size slightly bigger than $600 \mu\text{m}$ (i.e. 3×3 array), whereas in the simulated system N was 4. The MTF of the experimental system is calculated from the PSF data with a Fourier transformation and scaling [3].

MLAs used in the experimental setup are identical, and only the distances of MLAs are adjusted. As expected, compare to the simulated $f/5$ spherical system where focal lengths and distances of MLAs are optimized, the performance observed in the experiment is worse, due to both alignment errors and MLAs being constrained to be identical. Full scan line captures

are obtained from the experimental setup, with a long exposure time while the MLAs move. Figure 7(a) shows the discrete spots on the scan line captured while only the MMLA is scanned and Fig.7 (b) shows the full scan line captured while both the MMLA and PSL is scanned concurrently such that the phase condition defined in Ref. [2] is satisfied to maintain constructive interference at all scan angles. The tilt due to the PSL is a small fraction of the tilt introduced by the MMLA, thus, even though PSL focal length is much longer, the required PSL motion is still smaller than the MMLA motion.

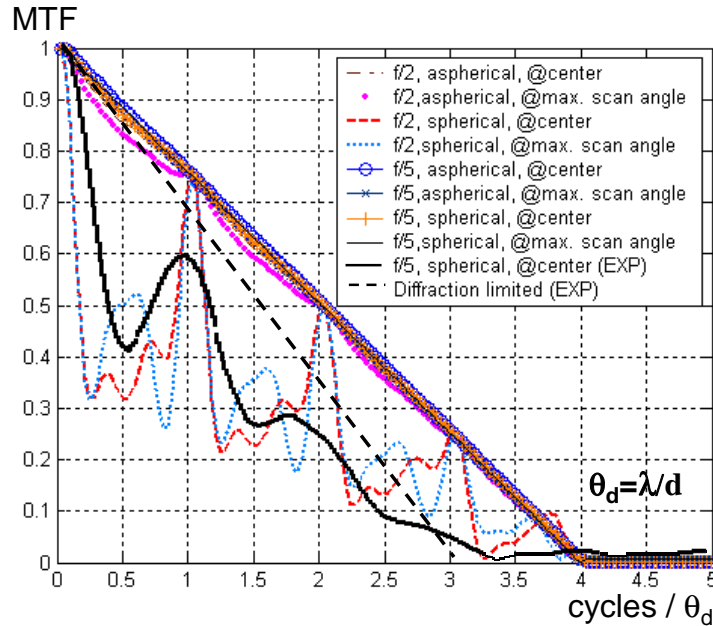


Fig. 6. Simulated MTF of the system (4x4 MLAs) for various configurations and MTF of the experimental system (3x3 square-packed 100% fill-factor MLAs), ($\theta_d = \lambda/d$, angular diffraction order separation)

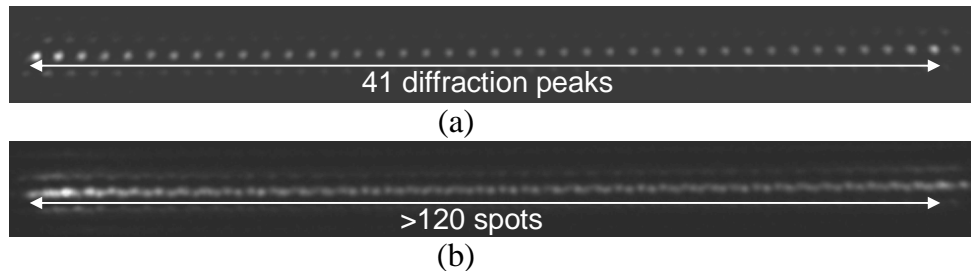


Fig. 7. Long exposure captures of line scanning using identical $f/5$ MLAs (a) MMLA moves, (b) both MMLA and PSL move synchronously. (from Ref. 2)

6. Conclusion

A ray-tracing and physical optics based hybrid method for optimization of telescopic array systems is reported. A high-resolution MLA beam steering system with continuous addressing ability is described. Assuming a clear aperture of 2 mm filled with 100 μ m pitch MLAs, 1880 \times 1880 resolution using $f/2$ aspherical MLAs and 752 \times 752 resolution using $f/5$ spherical MLAs are simulated. Experimental demonstration is successful using $f/5$ spherical MLAs and 600 μ m clear aperture. The system is suitable for endoscopic laser camera and agile beam steering applications.

This research is partly sponsored by EC-FP6 program NEMO network, TÜBİTAK grant 106E068, and TÜBİTAK Graduate Scholarship Program.